JACS
JOURNAL OF THE AMERICAN CHEMICAL SOCIETY
Article
pubs.acs.org/JACS

Single-Molecule Methods for Ligand Counting: Linking Ion Uptake to DNA Hairpin Folding

Andrew Dittmore,[†,⊥] Jonathan Landy,[†,§] Adrian A. Molzon,[†] and Omar A. Saleh*[,†,‡]

[†]Materials Department and [‡]BMSE Program, University of California, Santa Barbara, California 93106, United States

Supporting Information

ABSTRACT: Ligand associations play a significant role in biochemical processes, typically through stabilizing a particular conformation of a folded biomolecule. Here, we demonstrate the ability to measure the changes in the number of ligands associated with a single, stretched biomolecule as it undergoes a conformational change. We do this by combining thermodynamic theory with single-molecule measurements that directly track biomolecular conformation. We utilize this technique to determine the changes in the ionic atmosphere of a DNA hairpin undergoing a force-destabilized folding transition. We find that the number of counterions liberated upon DNA unfolding is a nonmonotonic function of the monovalent salt concentration of the solution, contrary to predictions from common nucleic acid models. This demonstrates that previously unobserved phenomena can be measured with our ligand counting approach.

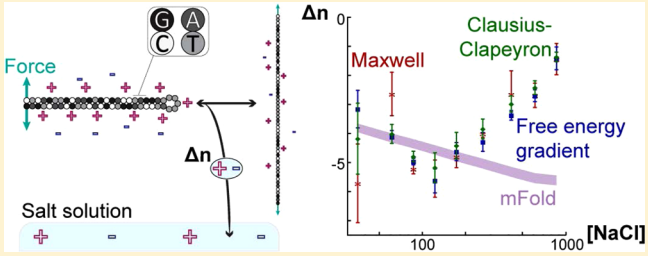

INTRODUCTION

The interaction of a ligand with its receptor is a fundamental biomolecular process whose quantification, in terms of stoichiometry and/or affinity, is the goal of a wide array of techniques of analytical biochemistry.[1] The effect of a ligand interaction is typically to alter the ensemble of available conformations of the receptor molecule, e.g., by favoring or inducing a high-affinity structure. Various single-molecule techniques provide direct access to, and even control of, biomolecular conformational fluctuations and are thus a direct means to investigate the effect of ligand interactions on the conformational ensemble of the receptor. Compared to traditional "bulk" assays, single-molecule approaches have the advantage of not averaging over multiple molecules, allowing access to sample heterogeneity and permitting quantification of time-dependent conformational trajectories. Indeed, this strategy has been applied to study ligand-dependent conformations of nucleic acid[2,3] and protein[4,5] receptors. This prior single-molecule work has mainly focused on the variation of receptor conformation with ligand concentration. Here, we show that such data sets can also be used to quantify the number of ligands interacting with a receptor molecule.

As a model system, we focus on the interaction of monovalent salt ions (the ligands) with a folded nucleic acid structure (the receptor). This system has the advantage of being experimentally accessible, since equilibrium conformational fluctuations of a small folded DNA hairpin can be tracked relatively easily. That said, studies of ion/nucleic acid systems also possess significant intrinsic merit: In aqueous solution, a negatively charged nucleic acid molecule is enshrouded by a local ion atmosphere with an anion depletion and cation enhancement. These local ion compositions vary with folding or upon complexation with another molecule.[6] Quantification of these local solute ions provides key information about the electrostatic contribution to folding, stability, and function in RNA and DNA.

Various bulk methods have previously been devised to quantify the ions associated with a nucleic acid; these methods supply complementary results with which to compare our approach. Direct bulk quantification of ions has been achieved through measurements that rely on spectroscopic signatures[7−9] or by using ion-specific fluorescent probes.[10] However, some of these approaches are limited to particular ions, and none give information on the variations in the ion atmosphere that accompany biomolecular configurational changes. An alternative approach is to characterize the ion atmosphere through a thermodynamic treatment.[11] Making use of certain assumptions, this approach has been widely used to estimate changes in the ion atmosphere upon thermal denaturation.[6] Such data have been used to generate the approximate salt- and temperature-dependent nearest-neighbor stability parameters in the predictive model of nucleic acid folding underlying the web server *mfold*;[12−14] this model provides a useful point of comparison for our results, as discussed below.

To quantify ion/nucleic acid interactions, we perform experiments using methods of single-molecule manipulation and interpret them within a rigorous thermodynamic framework. In the experiments, we perturb and read-out biomolecular conformation by directly applying force to a DNA hairpin and measuring the resulting extension. Such manipulation techniques are capable of providing refined

Received: January 6, 2014
Published: April 2, 2014

   dx.doi.org/10.1021/ja500094z | J. Am. Chem. Soc. 2014, 136, 5974−5980

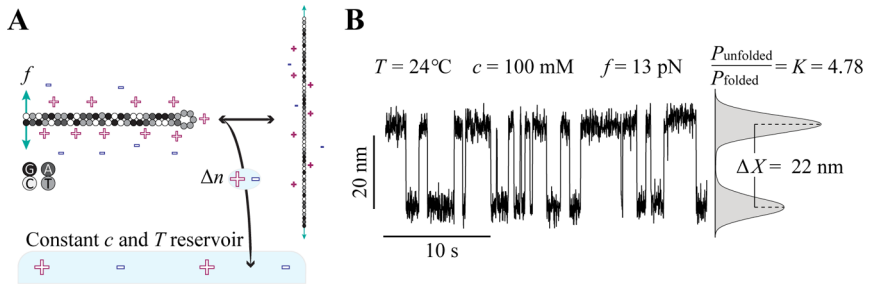

Figure 1. Method of single-molecule measurement of counterion excess changes in a two-state DNA hairpin. (A) Schematic of the DNA hairpin molecule in its aqueous ion environment. The local uptake/release of Δn excess counterions coincides with hairpin folding/unfolding at constant force f. Ion pairs exchange with the bulk solvent, an infinite reservoir at fixed monovalent salt concentration c and temperature T. (B) Representative time-series signal of molecular extension X. Temperature, salt concentration, and force are held constant during this measurement. The fraction of points in each of the two states determines the measured equilibrium constant $K(f,c) = P_{\text{unfolded}}/P_{\text{folded}}$, with uncertainty determined by the binomial sampling error. The difference in the median values of the folded and unfolded states provides a direct measurement of ΔX.

estimates of thermodynamic parameters[15,16] and have been used previously to investigate issues of nucleic acid electrostatics.[17−19] Direct manipulation measurements circumvent a major shortcoming of thermal denaturation experiments: the necessity for strong assumptions in the thermodynamic interpretation.[20] Whereas the analysis of thermal denaturation data is complicated by the fact that multiple free energy terms are affected by changes in temperature—often in ways that are still not fully understood—the free energy difference due to a change in applied force is always exactly characterized by a simple mechanical work term. In general, this enables an assumption-free thermodynamic analysis of single-molecule, force−extension data.

Here, using single-molecule manipulation with precise control of force, we gently guide the structure of a model DNA hairpin and cause a change in the ion atmosphere (Figure 1) whose composition is directly linked to molecular conformation.[21] Although the sum of the excess cations and missing anions is a constant defined by charge neutrality, the DNA draws in ions as it folds: To compensate for the increased charge repulsion between nucleotide phosphates, which are arranged at a higher density in the folded structure, the cation excess increases, and the anion deficit decreases. The process is reversed upon denaturation and ions dissociate from the molecule in charge neutral pairs. We measure changes in extension X covering the range of constant forces f for which the molecule appreciably visits the folded and unfolded states and repeat this measurement at several different concentrations c of monovalent salt.

With such data, we show that considerations of equilibrium thermodynamics enable multiple methods of quantifying conformation-induced changes in the ion atmosphere. We present three methods that rely on different experimental quantities: (1) The Maxwell relation method, in which the equilibrium extension $X(f,c)$, a smooth and continuous variable, is connected to ion release, $\Delta n(f,c)$, through the equivalence of mixed partial derivatives of free energy. The use of Maxwell relations in single-molecule studies was first suggested by Zhang and Marko.[22] (2) The Clausius−Clapeyron method, in which the variation with c and f of a two-state equilibrium condition permits estimate of Δn. (3) The free energy gradient method, in which Δn is estimated from the slope with c of the logarithm of the two-state equilibrium constant, $\ln K(c)$. We apply these methods to the data on hairpin unfolding and find that Δn exhibits a nonmonotonic variation with salt that is not anticipated by the *mfold* model.

Thermodynamic Framework. Our system comprises a stretched DNA molecule whose presence perturbs the concentration of ions relative to the bulk solution. These ions are free to diffusively exchange with the surrounding solvent, which to good approximation can be modeled as an infinite reservoir at some constant salt concentration. We define the volume, V, of the atmosphere to be large enough to contain all DNA-induced perturbations in solution conditions relative to the reservoir. The independent thermodynamic parameters are thus the force f stretching the DNA, the chemical potentials μ_i of the solute and solvent molecules, the temperature T, and the volume V. The proper free energy describing the system (DNA +environment) is the grand potential $\Omega(T, V, \mu_i, f) = U - TS - \sum_i \mu_i N_i$, where U is the energy, S the entropy, and N_i the total number of particles of species i. We seek the thermodynamic identity relating changes $d\Omega$ to changes in the experimentally varied parameters c and f (V and T are constant here). To do this, we follow Landy et al.,[23] as described in detail in the Supporting Information. Briefly, we apply a Gibbs−Duhem relation to relate the chemical potential of the solvent (water) to that of the solute (ions)[24] and relate changes in ion chemical potential to changes in c by introducing a coefficient α that accounts for possible nonideal behavior of the salt, where $\alpha = 1 + c(\partial/\partial c) \ln \gamma_{\pm}\beta$. In this expression, $\gamma_{\pm}$ is the mean activity coefficient of the salt ions (conventionally tabulated in molal units), and β is a factor accounting for the concentration-dependent molal/molar conversion. Note that $\alpha = 1$ in the limit of a dilute solution and that α deviates from unity by, at most, 10% over the relevant concentration range (see Supporting Information). Finally, we make use of the charge neutrality condition in the bulk ($c_+ = c_-$), which introduces a factor of 2 into the final expression. These considerations lead to the following identity, which underlies each ligand-counting method:

$$d\Omega = -2kTn_+\alpha d\ln c - Xdf \qquad (1)$$

where k is Boltzmann's constant, and n_+ is the excess cation number. The excess ion number is roughly the difference between the number of ions in V and the number in an equivalent volume of bulk solution.[23,24] The identity explicitly shows how changes in f and c affect the free energy of the system and consequently how they alter equilibria among various DNA conformations. Single-molecule measurements permit direct tracking of DNA conformation (here, through extension, X) and can thereby quantify equilibria through measurement of the probability of occurrence of various

dx.doi.org/10.1021/ja500094z | J. Am. Chem. Soc. 2014, 136, 5974−5980

conformations. Thus, eq 1 can be used to relate experimental estimates of f, X, c, and/or equilibria to changes in the counterion excess, n_+. This can be done in three ways (see Supporting Information for details).

Maxwell Relation Method. Maxwell relations originate from the insensitivity to order of differentiation of analytic (smooth) multivariable functions. Thus, assuming Ω smoothly varies with f and c, we find a Maxwell relation from eq 1 by equating mixed second derivatives and integrating to give an ion counting formula:[23,22]

$$\Delta n = n_+(f_2, c) - n_+(f_1, c) = \frac{1}{2kT\alpha}\int_{f_1}^{f_2}\left(\frac{\partial X}{\partial \ln c}\right)_f df \quad (2)$$

The output is a continuous change in n_+ over varying forces at constant c. We discuss the assumption of smoothness of Ω below.

Clausius–Clapeyron Method. For the other two methods, we assume our system has two separate, identifiable states, denoted by A and B; here, these are the folded and unfolded states of the hairpin, each with unique extensions X_A, X_B and ion-excesses $n_{+,A}$, $n_{+,B}$. By analogy to coexistence in a bulk phase transition, we can derive a Clausius–Clapeyron condition for the constraint on small changes to the system that do not modify the free energy difference $\Omega_B - \Omega_A$. This requires $d\Omega_A = d\Omega_B$, which from eq 1, leads to a relation for the ion excess difference between the two states:

$$\Delta n = n_{+,B}(f, c) - n_{+,A}(f, c) = \frac{X_A - X_B}{2kT\alpha}\left(\frac{\partial f}{\partial \ln c}\right)_{\ln K} \quad (3)$$

In a bulk phase transition, the Clausius–Clapeyron relation is strictly applied along the coexistence curve ($\Omega_B = \Omega_A$, or $\ln K = 0$). In the present microscopic system, observable fluctuations permit quantification of K away from coexistence and thus evaluation of $\partial f/\partial \ln c$ for any fixed values of the equilibrium constant.

Free Energy Gradient Method. Eq 1 directly indicates that the variation of free energy with c is connected to the ion excess through $(\partial\Omega/\partial \ln c)_f = -2kTn_+\alpha$. We can measure this free energy gradient by linking free energy to the equilibrium constant: $\Omega_B - \Omega_A = -kT\ln K = -kT\ln P_B/P_A$, where $P_{A,B}$ is the probability of observing each state. We arrive at a third counting formula:

$$\Delta n = n_{+,B}(f, c) - n_{+,A}(f, c) = \frac{1}{2\alpha}\left(\frac{\partial \ln K}{\partial \ln c}\right)_f \quad (4)$$

EXPERIMENT

We purchased a PAGE-purified DNA oligomer (Integrated DNA Technologies) that forms a hairpin structure with 25 base pairs in the stem sequence and an unpaired 5 nucleotide loop (Figure 1A). At either end of the stem, where unzipping initiates, abasic sites provide space between the hairpin and the tension-bearing handles.[25] At the 5′ end, we used a 15 nucleotide overhang sequence to attach a 1050 base-pair digoxigenin-terminated DNA handle generated using autosticky PCR,[26] while at the 3′ end, a 20 nucleotide overhang sequence formed a biotin-terminated DNA handle upon hybridization.

We diluted the annealed product to a nominal concentration of 50 pM and performed the final purification step *in situ*: We prepared a simple flow cell by adjoining a pair of glass coverslips using parafilm heated to 80 °C. The patterned parafilm also defined the dimensions of the channel (~0.2 × 5 × 40 mm). Digoxigenin antibodies densely adsorbed to the inner hydrophobic (SigmaCote, Aldrich) surface specifically immobilized the DNA, and only the correctly annealed product could capture a streptavidin-coated paramagnetic bead (Dynal, MyOne). The flow channel thus served as a purification chamber to isolate the correct product.

We controlled the solution conditions and performed all measurements at 24 °C in pH 7.5 Tris buffer including 0.1% Triton-X100 and Pluronic-F127; these nonionic surfactants prevent the beads from sticking to the flow-cell surface during buffer exchange. We varied the amount of NaCl salt dissolved in the buffer and ignored the insignificant contribution of Tris cations (~8 mM) in our reported values of c. We performed measurements at NaCl concentrations of 25, 50, 75, 100, 150, 200, 350, 500, 750, and 1000 mM and at constant forces ranging from 10 to 18 pN.

We used magnetic tweezers based on an inverted microscope at 50× magnification, and with motorized external magnets, to apply controlled pN-scale forces through DNA-tethered paramagnetic beads, while measuring DNA length through analysis of bead images.[27,28] The force for a given magnet position was calibrated using a Langevin analysis of the Brownian motion of beads tethered to long DNAs.[29] Using this approach leads to a systematic uncertainty in force of roughly 10% due to bead-to-bead variations. As discussed below, the agreement between various ligand-counting approaches lends confidence to our force-calibration procedure. Using the conditions described above, we found that the DNA molecules immobilized to the surface at an approximate density of 1 per 1000 μm^2. Beads tethered by multiple molecules were uncommon and easy to identify. Only single-molecule tethers showed the expected telegraphic signal over a narrow range of constant tensile forces (Figure 1B), consistent with stochastic transitions between the folded and unfolded states.

Data Analysis. For each time-series trace of extension values, we generated a histogram of length observation counts using 0.1 nm binning intervals, then fit a fourth-order polynomial to the logarithm of the histogram bin counts. The local minimum of the polynomial determined the threshold value between the two states. We then calculated the probability of each state (±binomial sampling error) as the fraction of points falling on either side of the threshold. The Clausius–Clapeyron counting method (eq 3) depends on the relative extension change. To measure the distance ΔX between states, we subtracted the median value of points in the unfolded state from that of the folded state and then took the median average across all time-series traces at the same salt concentration. For evaluation of the Maxwell relation (eq 2), we set the absolute extension of the hairpin in the folded state to zero and found the mean extension (±standard deviation) of each time series. We propagated the uncertainty estimates through all subsequent calculations.

The equilibrium constant is the ratio of fractional occupancies of the hairpin in the unfolded and folded states—a value that is independent of the measured extension. We applied local and first-order plane-fit smoothing in the array of $\ln K$ values across salt and force and then selected the points for which $|\ln K| \leq 3$. We evaluated the slopes between points at neighboring salt concentrations and at the same force and took the median of such slopes to find Δn using the free energy gradient method (eq 4). For the Clausius–Clapeyron method (eq 3), we evaluated the changes in force that maintained a constant $\ln K$ at neighboring salt concentrations by using a linear interpolation of the measured forces.

The phase diagram in the force-salt plane (Figure 2B) illustrates the free energy gradient (eq 4) and Clausius–Clapeyron (eq 3) ion counting procedures. We extend the conventional Clausius–Claperyon definition and evaluate the tangent to coexistence curves near, but not necessarily at, the phase boundary. Such curves represent the variations in f and c that maintain constant values of $\ln K$. The free energy gradient method involves evaluating constant-force slices across these contours.

Evaluation of the Maxwell-relation integral (eq 2) does not rely on a two-state model and returns curves of Δn vs force (Figure 3). For comparison with the other methods, we took Δn at its maximum magnitude for each value of c.

dx.doi.org/10.1021/ja500094z | J. Am. Chem. Soc. 2014, 136, 5974–5980

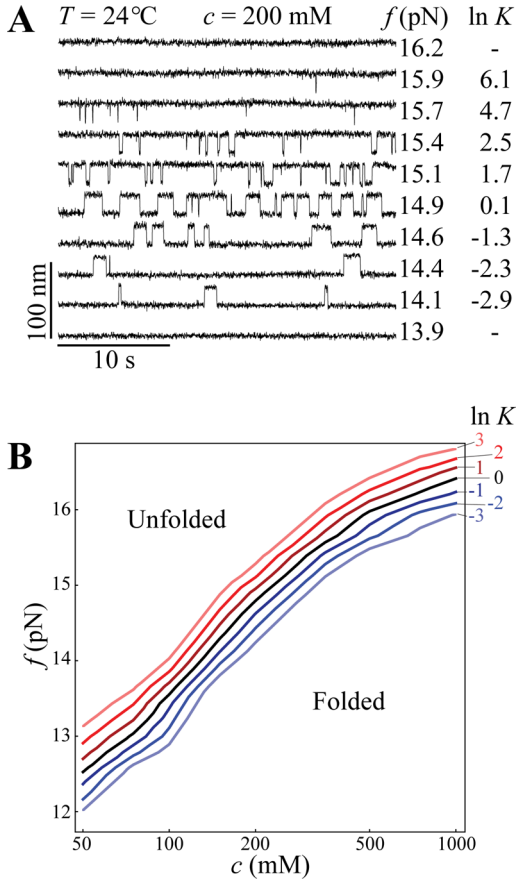

Figure 2. Representative data from a single DNA hairpin molecule. (A) Two-state dynamics at controlled forces and fixed solution conditions. From each time-series trace we extract the distance between states and the fractional occupancy in each state. (B) Force vs salt phase diagram of hairpin stability. Increasing force stabilizes the unfolded state, and increasing salt stabilizes the folded state. The black line indicates the equilibrium condition, $P_{folded} = P_{unfolded} \rightarrow \ln K = 0$. Other curves indicate changes in f and c that maintain coexistence at constant values of K, spanning the range $-3 \leq \ln K \leq 3$. The Clausius–Clapeyron method (eq 3) relies on evaluation of the slope of such coexistence curves, $(\partial f/\partial \ln c)_K$, while the free energy gradient method (eq 4) relies on evaluation of the gradient across curves at constant force, $(\partial \ln K/\partial \ln c)_f$.

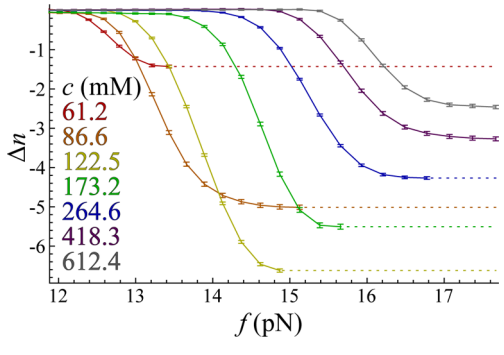

Figure 3. Ion release vs force for hairpin stretching at various salt concentrations. These curves are the output of evaluating the Maxwell-relation integral (eq 2). The method relies on measurement of the smooth and continuous change in the mean extension, $X(f, c)$. We took the minimum value of each curve (dashed lines) as the total Δn across the unfolding transition.

RESULTS

The three counting methods return measurements of Δn at each salt concentration that are, within error, indistinguishable (Figure 4A) . We find that Δn first increases in magnitude with c, up to [NaCl] ≈ 100 mM, and then steadily decreases in magnitude at higher values of c.

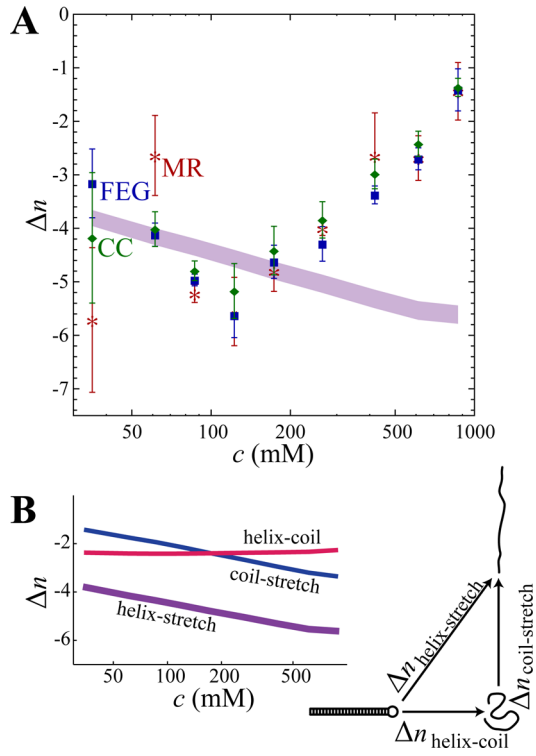

Figure 4. Ion counting by three methods in comparison to *mfold*: Maxwell-relation method (red), Clausius–Clapeyron method (green), and free energy gradient method (blue). Data points are the weighted mean (±sample standard deviation) for measurements repeated using three individual hairpin molecules. The shaded region represents the uncertainty envelope for the *mfold* prediction, including contributions from both $\Delta n_{helix-coil}$ and empirical $\Delta n_{coil-stretch}$ values. B) Schematic of two ion-release pathways. The path independence of thermodynamic states assures that $\Delta n_{helix-stretch} = \Delta n_{helix-coil} + \Delta n_{coil-stretch}$.

We compare our data with *mfold*, which predicts a value for the free energy difference between folded and unfolded states based on salt-dependent nearest-neighbor parameters of the free energy.[14] From this free energy difference, we can estimate Δn using the free energy gradient method. A complication is that *mfold* predicts thermodynamic properties of the transition from folded (helix) to unfolded (coil) states, while we measure a transition from the helix to an extended (stretch) state. We resolve this via the path independence of thermodynamic states: the total ion release we measure for the helix–stretch transition is the sum of two components (Figure 4 B): $\Delta n_{helix-stretch} = \Delta n_{helix-coil} + \Delta n_{coil-stretch}$. The first component includes the release of ions upon denaturation of the helix in the absence of force, at constant T = 24 °C and with c ranging from 25 to 1000 mM NaCl. Evaluation of the salt-dependent free energy output of *mfold* returns a constant $\Delta n_{helix-coil} = -2.2 \pm 0.1$ before applying the ion activity correction factor, $\alpha(c)$. The remaining ion release is due to single-stranded DNA stretching. In prior work, we quantified $\Delta n_{coil-stretch}$, finding it to increase in magnitude with salt concentration.[23] We thus can

dx.doi.org/10.1021/ja500094z | J. Am. Chem. Soc. 2014, 136, 5974–5980

compare the measured $\Delta n_{\mathrm{helix-stretch}}$ to that predicted from the sum of $\Delta n_{\mathrm{helix-coil}}$ from *mfold* and $\Delta n_{\mathrm{coil-stretch}}$ from single-stranded DNA stretching; this is shown in Figure 4.

For a two-state transition, we expect a sigmoidal dependence with force of the probability to observe either state. This suggests that the equilibrium constant will vary as $\ln K = -(f - f_{1/2})\Delta X/kT$, where $f_{1/2}(c)$ is the equilibrium force. We use this as a check on our experimental measurements: Direct quantification of the length of the folded and unfolded states indicates $\Delta X = 22.4 \pm 0.3$ nm, while fitting to the expected two-state behavior of K gives $\Delta X = 21.9 \pm 0.3$ nm (median ± sample standard deviation across c). These values are statistically equivalent, lending confidence to our experimental ability to quantify length, force, and the equilibrium constant. Note, however, that the best-fit sigmoidal dependence was not utilized in any estimates of Δn, which relied directly on the data without any intermediary global fitting steps.

DISCUSSION

Single-Molecule Ligand-Counting Thermodynamics. We have presented three equations, eqs 2−4, that permit estimate of the number of ions surrounding a single tethered, stretched biomolecule; note that the Maxwell method (eq 2) has been presented previously.[22,23] The precise form of the equations given is specific to monovalent salt solutions through the use of charge neutrality in their derivation. However, they can be broadly applied to count neutral ligands interacting with the manipulated molecule simply by removing the factors of two in eqs 1−4.

Each counting method has its advantages and drawbacks. We base the free energy gradient and Clausius−Clapeyron methods on a two-state assumption, which relies on the ability to correctly identify two states in the data. These methods could be extended to systems with additional states if they can be robustly identified in the measurement. In this sense, the Maxwell relation is the most general, as it makes no assumptions about the number of states in the system and so can be applied without alteration to multistate transitions. The Maxwell relation requires only that the free energy is a smooth function of f and c, which is not a significant barrier: In bulk, two-state phase transitions are marked by sudden (not smooth) changes in thermodynamic parameters; however, in microscopic systems, two-state transitions are smoothed by fluctuations, permitting broad application of the Maxwell relation. This is the case for our system, where the Maxwell method gave statistically identical results to the other two methods.

From a theoretical perspective, the three counting methods are equivalent and amount to different methods of analyzing free-energy differentials. However, each method makes use of the experimental data in a different way; thus, the three methods can give different results due to variations in the quality of different experimental parameters. For example, the Clausius−Clapeyron method makes use of all measured parameters, i.e., both the f and $X_{A,B}$ values, but these can be offset by systematic errors in a poorly calibrated system. The free energy gradient method does not explicitly require either f or X values so is robust against such systematic error in estimates of those parameters. This broadens the applicability of this approach to methods, such as FRET, that can resolve two-state equilibria, but do not directly measure microscopic lengths nor apply force. However, the free energy gradient approach does require precise determination of K, which might require sampling of rare, fast transitions. Considering these differences in the counting procedures, the close agreement we measure in Δn between the Clausius−Clapeyron and free energy gradient methods indicates that we are accurately measuring both force and length.

In practice, we found the Maxwell relation is the most difficult to apply: the integration inherent to the process can compound errors, particularly if the measurement of X is affected by drift (a common issue in single-molecule experiments). In comparison, the two-state assumption of the other two methods makes them intrinsically differential and thus highly robust against drift. For a quality data set, the three methods, although based on different experimental quantities, should provide nearly the same information and serve as an internal consistency check. Our experiments on the DNA hairpin system demonstrate that identical information can indeed be extracted from each method (Figure 4).

The Nonmonotonic Trend in Ion Release: Changes in Molecular Compactness in the Helix and Stretch States. All three analysis methods agree that ion release upon mechanically unfolding a DNA hairpin is nonmonotonic with salt concentration, particularly with $\Delta n_{\mathrm{helix-stretch}}$ peaking at $c \approx 100$ mM. Qualitatively, this nonmonotonic trend can be easily discerned from the behavior of the phase boundary (Figure 2B), which has a steep slope for intermediate c and weaker slopes at the extremes, since the Clausius−Clapeyron method (eq 3) indicates the ion release is proportional to that slope.

We seek a physical explanation of the nonmonotonic behavior. Generally, we expect the total counterion excess, n_+, to be sensitive to both structural rearrangements of the molecule and charge screening from the background salt. To isolate the background-screening effect, imagine a DNA structure that is static, with a fixed density of phosphate charges. Then n_+ would decrease with increasing c; fewer excess counterions would be required as the concentration of background salt takes over the task of charge screening. Put another way: at higher c, the screening length decreases, so a fixed conformational state will look to the ions like it is effectively becoming less compact, decreasing n_+.

We next consider the effect of salt in altering the ensemble average conformation of each state. Generally, higher salt will increase the compactness of charged molecules, as the decreased screening length reduces intramolecular electrostatic repulsion. The resulting compact conformations have higher charge densities that absorb more ions from the bulk; importantly, this conformational effect will contribute an increase in n_+ with c that counteracts the attenuation due to background screening.

For each individual state (helix, coil, stretch), the absolute counterion excess n_+ will depend on the competing contributions of background screening and salt-dependent conformation. For the stretch state, experiments show that the compactness increases slowly and continuously with c, as seen in measurements of the weak salt dependence of the length of single-stranded nucleic acids for $f > 10$ pN.[17,30] Thus, for the stretch state, we expect a net decrease in n_+ with c, due to the dominance of the background screening effect over the weak compaction; this is sketched in Figure 5. Given a decrease of $n_{+,\mathrm{stretch}}$ with c, our measurements of $\Delta n_{\mathrm{helix-stretch}}$ indicate that $n_{+,\mathrm{helix}}$ is roughly constant (or perhaps slowly increases) for $c <$ 100 mM and then decreases with c above 100 mM. This is consistent with the helix state (the folded hairpin) becoming more compact with salt for small c, where the effects of

dx.doi.org/10.1021/ja500094z | J. Am. Chem. Soc. 2014, 136, 5974−5980

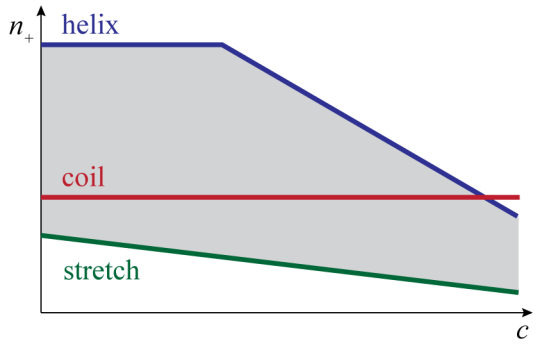

Figure 5. Qualitative sketch of absolute ion excess, n_+, for each state of the DNA hairpin: helix, coil, and stretch. Our measurement is of $\Delta n_{\text{helix}-\text{stretch}}$, colored in gray. For low salt, the curves are ordered by charge density, since higher charge densities will create a larger ion excess. The relative trend of each state with salt is determined by comparison to experiments; see text for details.

compaction and background screening roughly cancel, then having a conformation independent of salt at high c, where background screening dominates. Consistent with this apparent conformational behavior, double-stranded DNA is known to have a persistence length that decreases for low salt but is relatively constant beyond $c \approx 100$ mM,[31] which would cause the hairpin stem to become more compact with c in the low-salt regime, then asymptote to a constant conformational ensemble at higher salt. Alternatively, the conformational ensemble of the hairpin loop could transition with c from a salt-induced compaction to salt insensitivity, with the crossover occurring as the solution screening length decreases through the finite extent of the loop. While more experiments are needed to separate the contribution of stem and loop to $n_{+,\text{helix}}$, the posited microscopic mechanisms plausibly explain the shape of the $n_{+,\text{helix}}$ vs c curve (Figure 5). Finally, we note that Bai et al.[9] utilized atomic emission spectroscopy to directly quantify n_+ vs c for a 24 bp double-helical DNA, similar in length to the stem of the hairpin used here. Their results are qualitatively similar to the sketch of $n_{+,\text{helix}}$ in Figure 5, lending confidence to our interpretation.

The Behavior of the Coil State and Comparison to Bulk Experiments. In contrast to the behavior of the helix and stretch states, the conformation of the tension-free coil state will strongly vary with salt. In particular, at high-salt concentrations, the decreased screening length allows the coil to take on more compact conformations with sharper bends and a lower energetic cost for ion uptake.[21,23] This compaction effect will contribute an increase in n_+ with c that counteracts the decrease in n_+ due to background screening. *A priori*, it is difficult to predict which effect will dominate. However, prior measurements indicate $\Delta n_{\text{coil}-\text{stretch}}$ increases with c.[23] Given $n_{+,\text{stretch}}$ slowly decreasing with c, this means $n_{+,\text{coil}}$ is at least constant with c and perhaps slowly increasing (Figure 5). This prediction could be tested by repeating the experiment of Bai et al.[9] for a short unstructured ssDNA.

The above considerations, based on the presented data for $\Delta n_{\text{helix}-\text{stretch}}$ and prior data on $\Delta n_{\text{coil}-\text{stretch}}$,[23] lead to the prediction that $\Delta n_{\text{helix}-\text{coil}}$ will be roughly constant for $c < 100$ mM but decrease with salt for $c > 100$ mM. Bulk, tension-free experiments are sensitive to $\Delta n_{\text{helix}-\text{coil}}$, which is the parameter that determines the salt dependence of the folding free energy of the hairpin. We do find agreement between our prediction of $\Delta n_{\text{helix}-\text{coil}}$ and some bulk measurements; particularly studies where DNA melting data are treated using a version of the free energy gradient method in which derivatives are evaluated at constant temperature.[32] However, whereas the behavior we expect for $\Delta n_{\text{helix}-\text{coil}}$ is consistent with that derived from the popular *mfold* software package for $c \leq 100$ mM, it is not consistent at higher salt. The *mfold* program is based on nearest-neighbor stability parameters derived from a comprehensive experimental data set on DNA melting.[12] Given the specific solution conditions and primary DNA sequence, *mfold* returns values for, among other things, the Gibbs free energy difference, ΔG, between the helix and coil states. Evaluation of $\partial\ \Delta G/\partial\ \ln c$ at $T = 24$ °C gives a constant value for $\Delta n(c)_{\text{helix}-\text{coil}}$, in contrast to our measurements and others.[32] This discrepancy indicates that, although *mfold* does an excellent job of predicting melting temperatures, other thermodynamic quantities may be problematic. Specifically, the electrostatic contribution to DNA stability is overestimated at high concentrations of NaCl.

We attribute the discrepancy between our results and predictions from *mfold* to the complexity of extrapolating thermodynamic quantities from thermal denaturation measurements. In this experiment, we hold the temperature constant; denaturation arises from the combined destabilizing effects of large forces and low-salt chemical potentials (which deprive the folded state of ions that screen the interstrand repulsion). Unlike measurements in which temperature drives unfolding, our use of force to directly denature the DNA avoids ambiguity in the interplay of thermodynamic quantities. Notably, force and chemical potential are truly independent of one another, whereas temperature variation also varies the chemical potential of the ions. Thermal variation can also have a wide variety of effects in a complex aqueous solution, e.g., by altering water structure. Thus, force is a more direct and incisive parameter whose effects can be interpreted with fewer assumptions.

■ CONCLUSION

We have presented theoretical methods that relate single-molecule manipulation data to the stoichiometry of ligands interacting with the manipulated biomolecule. These methods can be directly applied to any biomolecule/ligand interaction, so long as the equilibrium dynamics of the system are experimentally accessible. To apply and test these methods, we have focused on the nonspecific ion interactions of a folded DNA hairpin and found a nonmonotonic ion release trend upon unfolding the hairpin at different salt concentrations. This result is well substantiated by the close agreement between three different data analysis procedures. We attribute the disagreement with prior bulk measurements to subtleties in the interpretation of thermal denaturation data, in comparison to the relative simplicity of interpreting mechanical denaturation.

The single-molecule manipulation and analysis techniques presented here may be used by investigators in solving significant problems in RNA chemistry. The information gained will contribute to our understanding of RNA folding, function, and dynamics, particularly the relationship between structure, stability, and electrostatics. The methodology can be extended to systems involving multivalent salts or nucleic acids that fold through multiple states. The precision of the thermodynamic framework enabled by single-molecule manipulation may improve the predictive abilities of theories[19,33] or models such as *mfold*.

The methods described here are limited to manipulation experiments in which the equilibrium extension behavior can be

dx.doi.org/10.1021/ja500094z | J. Am. Chem. Soc. 2014, 136, 5974−5980

ascertained. This condition is met when working with relatively small hairpin nucleic acid structures. However, a variety of works have shown that only nonequilibrium mechanical unfolding trajectories can be accessed for more complex structures, such as, e.g., RNA pseudoknots.[34] It is likely that the theory we present can be modified to be applicable to such situations; notably, theoretical work has shown that the equilibrium free energy difference, $\Delta\Omega$, can be recovered from nonequilibrium pulling experiments, i.e., through application of the Jarzynski[35,36] or Crooks[37] relations. If such nonequilibrium experiments are repeated at a variety of ligand concentrations, then variation of $\Delta\Omega$ with ligand concentration can be analyzed with the free-energy gradient method to give Δn for the studied process.

■ ASSOCIATED CONTENT

Supporting Information

Supporting Information includes details of the thermodynamic derivation, along with the nonideal solution correction values. This material is available free of charge via the Internet at http://pubs.acs.org.

■ AUTHOR INFORMATION

Corresponding Author

saleh@engineering.ucsb.edu

Present Addresses

[⊥]Laboratory of Molecular Biophysics, NHLBI, National Institutes of Health, Bethesda, Maryland 20892, United States. [§]Chemistry Department, University of California, Berkeley, California 94720, United States.

Notes

The authors declare no competing financial interest.

■ ACKNOWLEDGMENTS

This work was supported by the National Science Foundation under grant no. DMR-1006737. We thank David Draper for helpful conversations. J.L. acknowledges support from NSF grants no. DMR-1101900 and CHE-1265664.

■ REFERENCES

(1) Klotz, I. *Ligand-receptor energetics: A guide for the perplexed*; Wiley: New York, 1997.
(2) Greenleaf, W. J.; Frieda, K. L.; Foster, D. A. N.; Woodside, M. T.; Block, S. M. *Science* **2008**, *319*, 630−633.
(3) Ha, T.; Zhuang, X.; Kim, H. D.; Orr, J. W.; Williamson, J. R.; Chu, S. *Proc. Natl. Acad. Sci. U.S.A.* **1999**, *96*, 9077−9082.
(4) Kim, E.; Lee, S.; Jeon, A.; Choi, J. M.; Lee, H.-S.; Hohng, S.; Kim, H.-S. *Nat. Chem. Biol.* **2013**, *9*, 313−318.
(5) Stigler, J.; Rief, M. *Proc. Natl. Acad. Sci. U.S.A.* **2012**, *109*, 17814−17819.
(6) Record, M. T.; Anderson, C. F.; Lohman, T. M. *Q. Rev. Biophys.* **1978**, *11*, 103−178.
(7) Walter, S. R.; Young, K. L.; Holland, J. G.; Gieseck, R. L.; Mirkin, C. A.; Geiger, F. M. *J. Am. Chem. Soc.* **2013**, *135*, 17339−17348.
(8) Das, R.; Mills, T. T.; Kwok, L. W.; Maskel, G. S.; Millett, I. S.; Doniach, S.; Finkelstein, K. D.; Herschlag, D.; Pollack, L. *Phys. Rev. Lett.* **2003**, *90*, 188103.
(9) Bai, Y.; Greenfeld, M.; Travers, K. J.; Chu, V. B.; Lipfert, J.; Doniach, S.; Herschlag, D. *J. Am. Chem. Soc.* **2007**, *129*, 14981−8.
(10) Grilley, D.; Soto, A. M.; Draper, D. E. *Proc. Natl. Acad. Sci. U.S.A.* **2006**, *103*, 14003−14008.
(11) Leipply, D.; Lambert, D.; Draper, D. E. *Methods Enzymol.* **2009**, *469*, 433−463.
(12) SantaLucia, J. *Proc. Natl. Acad. Sci. U.S.A.* **1998**, *95*, 1460−1465.
(13) SantaLucia, J.; Hicks, D. *Annu. Rev. Biophys. Biomol. Struct.* **2004**, *33*, 415−440.
(14) Zuker, M. *Nucleic Acids Res.* **2003**, *31*, 3406−3415.
(15) Vieregg, J.; Cheng, W.; Bustamante, C.; Tinoco, I. *J. Am. Chem. Soc.* **2007**, *129*, 14966−14973.
(16) Huguet, J. M.; Bizarro, C. V.; Forns, N.; Smith, S. B.; Bustamante, C.; Ritort, F. *Proc. Natl. Acad. Sci. U.S.A.* **2010**, *107*, 15431−15436.
(17) Anthony, P. C.; Sim, A. Y.; Chu, V. B.; Doniach, S.; Block, S. M.; Herschlag, D. *J. Am. Chem. Soc.* **2012**, *134*, 4607−4614.
(18) Bizarro, C. V.; Alemany, A.; Ritort, F. *Nucleic Acids Res.* **2012**, *40*, 6922−6935.
(19) Einert, T. R.; Netz, R. R. *Biophys. J.* **2011**, *100*, 2745−2753.
(20) Sharp, K. *Protein Sci.* **2001**, *10*, 661−667.
(21) Landy, J.; McIntosh, D.; Saleh, O.; Pincus, P. *Soft Matter* **2012**, *8*, 9368−9375.
(22) Zhang, H. Y.; Marko, J. F. *Phys. Rev. E* **2008**, *77*, 031916.
(23) Landy, J.; McIntosh, D. B.; Saleh, O. A. *Phys. Rev. Lett.* **2012**, *109*, 048301.
(24) Parsegian, V. A.; Rand, R. P.; Rau, D. C. *Proc. Natl. Acad. Sci. U.S.A.* **2000**, *97*, 3987−3992.
(25) Woodside, M. T.; Behnke-Parks, W. M.; Larizadeh, K.; Travers, K.; Herschlag, D.; Block, S. M. *Proc. Natl. Acad. Sci. U.S.A.* **2006**, *103*, 6190−6195.
(26) Gal, J.; Schnell, R.; Szekeres, S.; Kalman, M. *Mol. Gen. Genet.* **1999**, *260*, 569−573.
(27) Gosse, C.; Croquette, V. *Biophys. J.* **2002**, *82*, 3314−3329.
(28) Ribeck, N.; Saleh, O. A. *Rev. Sci. Instrum.* **2008**, *79*, 094301.
(29) Lansdorp, B. M.; Saleh, O. A. *Rev. Sci. Instrum.* **2012**, *83*, 025115.
(30) Saleh, O. A.; McIntosh, D. B.; Pincus, P.; Ribeck, N. *Phys. Rev. Lett.* **2009**, *102*, 068301.
(31) Baumann, C. G.; Smith, S. B.; Bloomfield, V. A.; Bustamante, C. *Proc. Natl. Acad. Sci. U.S.A.* **1997**, *94*, 6185−6190.
(32) Owczarzy, R.; Dunietz, I.; Behlke, M. A.; Klotz, I. M.; Walder, J. A. *Proc. Natl. Acad. Sci. U.S.A.* **2003**, *100*, 14840−14845.
(33) Denesyuk, N. A.; Thirumalai, D. *J. Phys. Chem. B* **2013**, *117*, 4901−4911.
(34) Ritchie, D. B.; Foster, D. A. N.; Woodside, M. T. *Proc. Natl. Acad. Sci. U.S.A.* **2012**, *109*, 16167−16172.
(35) Jarzynski, C. *Phys. Rev. E* **1997**, *56*, 5018−5035.
(36) Jarzynski, C. *Phys. Rev. Lett.* **1997**, *78*, 2690.
(37) Crooks, G. E. *Phys. Rev. E* **1999**, *60*, 2721−2726.